purification. All NMR spectra were obtained on a Varian XL-400 spectrometer operating at 399.93 MHz for ^{1}H and 100.56 MHz for ^{13}C at a probe temperature of 18 ± 1 °C. Unless otherwise indicated, spectra were obtained for 0.4 M solutions of hydrocarbon in the appropriate solvent.

Heteronuclear shift-correlated spectra were obtained with a version of this experiment that provides ^{1}H–^{1}H decoupling.[21] Typical spectra were obtained with a 240-Hz spectral width in the f_1 (^{1}H) domain and 2000-Hz spectral width for f_2 (^{13}C). Forty time increments were used with zero-filling in 256 in f_1 while 2048 data points were collected in f_2 with zero-filling to 4096. Sixty-four transients were collected for each time increment and, with a relaxation delay of 1.0 s between increments, total measuring time was 1.1 h. Pseudoecho processing[22] was applied in both domains to ensure maximum resolution. Repeat measurements indicated that ^{1}H chemical shifts could usually be determined with a precision of 0.005 ppm, i.e., 2 Hz.

Acknowledgment. Financial support from the Natural Sciences and Engineering Research Council of Canada in the form of a strategic grant (W.F.R. and M.A.W.), operating grants (W.F.R. and M.A.W.) and an International Scientific Exchange Award (R.G.E.) are gratefully acknowledged. R.G.E. also acknowledges financial support from CONACYT (Mexico).

Registry No. $C_{16}H_{34}$, 544-76-3; $C_{12}H_{26}$, 112-40-3; $C_{10}H_{22}$, 124-18-5; C_8H_{18}, 111-65-9; eicosane, 112-95-8; 1-chloronaphthalene, 90-13-1; 1-methylnaphthalene, 90-12-0.

References and Notes

(1) Liu, R. J. *J. Polym. Sci., Part A-2* **1967**, *5*, 1209.
(2) Lui, R. J. *J. Polym. Sci., Part A-2* **1968**, *6*, 947; *Macromolecules* **1968**, *1*, 213; *Polymer* **1969**, *10*, 951.
(3) Ando, I.; Nishioka, A. *Makromol. Chem.* **1972**, *152*, 7; **1972**, *160*, 145; **1973**, *171*, 195.
(4) Ando, I.; Nishioka, A.; Kondo, M. *Bull. Chem. Soc. Jpn.* **1974**, *47*, 1097.
(5) Gonzalez de la Campa, J. I.; Barrales-Rienda, J. M.; Gonzalez Ramos, J. *Macromolecules* **1977**, *10*, 989.
(6) Winnik, M. A.; Mar, A.; Reynolds, W. F.; Dais, P.; Clin, R.; Caussade, B. *Macromolecules* **1979**, *12*, 257.
(7) Gonzalez de la Campa, J. I.; Barrales-Rienda, J. M., *Polym. J. (Tokyo)* **1980**, *21*, 1372.
(8) Grant, D. M.; Cheney, B. V. *J. Am. Chem. Soc.* **1967**, *89*, 5315.
(9) Tonelli, A. *Macromolecules* **1976**, *9*, 863.
(10) Ando, I.; Inoue, Y. *Makromol. Chem., Rapid Commun.* **1983**, *4*, 753.
(11) Bax, A.; Morris, G. A. *J. Magn. Reson.* **1981**, *42*, 501.
(12) Stothers, J. B. "Carbon-13 NMR Spectroscopy"; Academic Press: New York, 1972.
(13) Freeman, R.; Hill, H. D. W. *J. Chem. Phys.* **1970**, *53*, 4103.
(14) Ando, I.; Nishioka, A. *Bull. Chem. Soc. Jpn.* **1973**, *46*, 1040.
(15) Rummens, F. H. A.; Krystynak, R. H. *J. Am. Chem. Soc.* **1972**, *94*, 6914. These authors show that there is a medium shift of −0.48 ppm for tetramethylsilane on going from chloroform to benzene. Similar results are expected for other aromatic solvent molecules.
(16) Chiang, R. *J. Chem. Phys.* **1966**, *70*, 2348.
(17) Lamotte, M.; Lesclaux, R.; Merle, A. M.; Joussot-Dubien, J. *Discuss. Faraday Soc.* **1974**, *58*, 253.
(18) Groszek, A. J. *Proc. R. Soc. London, Ser. A* **1970**, *314*, 473.
(19) This likely reflects, in part, different ASIS for the reference tetramethylsilane in the different aromatic solvents (see ref 15).
(20) Randall, J. C. "Polymer Sequence Distribution: Carbon-13 NMR Method"; Academic Press: New York, 1977.
(21) Bax, A. *J. Magn. Reson.* **1983**, *53*, 517.
(22) Bax, A.; Freeman, R. *J. Magn. Reson.* **1981**, *44*, 542.

Matrix Effects on the Diffusion of Long Polymer Chains[†]

Peter F. Green and Edward J. Kramer*

Department of Materials Science and Engineering and the Materials Science Center, Cornell University, Ithaca, New York 14853. *Received August 29, 1985*

ABSTRACT: The diffusion of long chains of molecular weight M (M-chains) into matrices of molecular weight P is studied by forward-recoil spectrometry. The matrix molecular weight P ranged from very short unentangled chains below the critical molecular weight for entanglement M_c to long highly entangled chains. Whereas the tracer diffusion coefficient D^* of the M-chains is independent of P for sufficiently large P in the entangled regime ($D^* \sim M^{-2}$), it rapidly increases with decreasing P for P less than a characteristic molecular weight P^* which increases slowly with M. This behavior is consistent with theoretical predictions that $D^* = D_{rep} + D_{cr}$. Here D_{rep} is the diffusion coefficient due to the reptation of the M-chain, and D_{cr} is an additional matrix contribution to the diffusion of the M-chain that arises from the simultaneous diffusion of the surrounding P-chains (constraint release). We find that D_{cr} scales approximately as $M^{-1}P^{-3}$. In the unentangled regime ($P < M_c$) studies were conducted at different temperatures where the fractional free volume of each matrix was equal to a constant, 0.042. Here the tracer diffusion coefficient scales approximately as $D^* \sim M^{-(0.5-0.6)}P^{-1}$, a result that is consistent with the chain diffusing as a coil of hydrodynamic radius $R \sim M^{-(0.5-0.6)}$ in a viscous environment whose viscosity scales as P.

Introduction

Current theories predict that the center of mass diffusion of a polymer chain of molecular weight M in an entangled polymer matrix of molecular weight P may occur by three different processes: reptation,[1,2] constraint release (tube renewal),[3-6] or Stokes–Einstein[5,6] diffusion. Which type of behavior is observed is expected to depend on the values of P and M.

The theory of Doi and Edwards[7] predicts that the diffusion of the chain of molecular weight M (M-chain) in a high molecular weight matrix occurs by reptation. Here motion of the chain is restricted to a tubelike region that is defined by the topological constraints of the neighboring matrix chains. As it crawls along the primitive path that its "tube" defines, its lateral motions are assumed to be prohibited on the time scale $\tau_{rep}(M) \sim M^3$, the time for it to diffuse out of the tube. If the constraints defining this tube remain relatively immobile on the time scale $\tau_{rep}(M)$, then the tracer diffusion coefficient D^* of this chain depends only on its molecular weight M so that

$$D^* = D_{rep}(M) = D_0 M^{-2} \tag{1}$$

where D_0 is independent of M. There is considerable experimental evidence that supports this prediction.[8-15]

[†] Materials Science Center Report No. 5634.

0024-9297/86/2219-1108$01.50/0

Of course, when the matrix chains become sufficiently short, eq 1 no longer provides an adequate description of the motion of the chain since the topology of the "tube" is being modified on time scales less than $\tau_{\mathrm{rep}}(M)$. Here modification of the "tube" occurs by the diffusion of the neighboring matrix chains away from the points at which they provide constraint. Such diffusion of the M-chains by motion of the P-chains surrounding the tube is called constraint release or tube renewal.

Graessley[3] has modified the Doi-Edwards model to allow constraint release to be modeled quantitatively. The matrix is approximated by a "lattice" of chains. Each chain independently reptates along its own primitive path. The linear dimensions of a cell in the lattice are equivalent to the length of a step on the primitive path. An M-chain of N primitive steps thus occupies N cells on the "lattice". Each cell is surrounded by z bars or "suitably situated" constraints corresponding to the matrix chains on the lattice. Here each bar represents a chain segment one primitive step in length.

The primitive path of the diffusing chain is altered when one of the segments on the M-chain undergoes a lateral displacement into an adjacent cell on the "lattice". This is facilitated by the removal of one of the z bars via diffusion of a suitably situated constraint away from that region. The diffusion coefficient that is predicted to arise from this constraint release mechanism is

$$D_{\mathrm{cr}} = \alpha_{\mathrm{cr}} D_0 M_{\mathrm{e}}^2 M^{-1} P^{-3} \tag{2}$$

where $\alpha_{\mathrm{cr}} = (48/25)z(12/\pi^2)^{z-1}$ and M_{e} is the molecular weight between entanglements. The parameter D_0 is the same constant that appears in D_{rep}, eq 1, and depends only on M_{e} and the Rouse mobility[16] of the diffusing chain. Since reptation and constraint release are independent mechanisms, the tracer diffusion coefficient of the M-chain may be written as

$$D^* = D_{\mathrm{rep}}(M) + D_{\mathrm{cr}}(M,P) = D_{\mathrm{rep}}(1 + \alpha_{\mathrm{cr}} M_{\mathrm{e}}^2 M P^{-3}) \tag{3}$$

An alternate approach adopted by Klein[5] yields a slightly different dependence of D_{cr} on P. The M-chain is treated as a Rouse chain with M/M_{e} independent submolecules. The total number of "tube" constraints per M_{e} is treated as one effective constraint. Whereas in the Graessley model the constraints are assumed to be independent, Klein argues that only a fraction of these, $(P/M_{\mathrm{e}})^{1/2}$, are in fact independent since it is likely that different segments on the same P-chain provide constraints at different points along the M-chain. It follows that the relaxation rate of constraints ought to be enhanced by a factor of $(P/M_{\mathrm{e}})^{1/2}$. The diffusion coefficient for this nonindependent constraint release (nicr) mechanism scales as

$$D_{\mathrm{nicr}}(M,P) \sim M_{\mathrm{e}}^{3/2} M^{-1} P^{-5/2} \tag{4}$$

which, if the numerical factors are ignored, differs from the second term in eq 3 by only the factor of $(P/M_{\mathrm{e}})^{1/2}$. Therefore, by including an unspecified constant K, we may write

$$D^* = D_{\mathrm{rep}}(1 + K M_{\mathrm{e}}^{3/2} M P^{-5/2}) \tag{5}$$

In the limit of very large M/P the motion of the M molecular weight chain may no longer be free draining, as is implicitly assumed in the models discussed above, and hydrodynamic interactions between M-chain segments (as discussed in the Zimm model[17]) may be important.[4] Under these conditions eq 2 should be replaced by

$$D_{\mathrm{SE}} \sim M_{\mathrm{e}}^{3/2} M^{-1/2} P^{-3} \tag{6}$$

and thus

$$D^* = D_{\mathrm{rep}}(1 + K' M^{3/2} M_{\mathrm{e}}^{3/2} P^{-3}) \tag{7}$$

where K' is an undetermined constant.

Daoud and de Gennes[6] arrive at a similar result by considering that in this limit the M-chain should diffuse as a coil of hydrodynamic radius $R(M) \sim M^{1/2}$ in a viscous medium whose viscosity is given by $\eta \sim P^3$. Consequently, the second term in eq 3 should be replaced by the Stokes–Einstein diffusion coefficient

$$D_{\mathrm{SE}} = k_{\mathrm{B}}T/6\pi\eta(P)R(M) \sim M^{-1/2}P^{-3} \tag{8}$$

where k_{B} is Boltzmann's constant.

The Daoud–de Gennes argument can be generalized to diffusion in unentangled matrices ($P < M_{\mathrm{c}}$). In this regime $\eta(P)$ scales as P, not P^3 or $P^{3.4}$. Hence the diffusion of a hydrodynamically screened (Rouse) tube (whose length $L \sim M$) in the unentangled viscous matrix should scale as

$$D_{\mathrm{uR}} \sim M^{-1}P^{-1} \tag{9}$$

A tube that is not hydrodynamically screened (Zimm) should diffuse as a coil of radius $R(M) \sim M^{1/2}$; hence, for this case

$$D_{\mathrm{uSE}} = k_{\mathrm{B}}T/6\pi\eta(P)R(M) \sim M^{-1/2}P^{-1} \tag{10}$$

If the P-chains are short enough, they should act as a good solvent for the M-chains.[2] The transition from Θ-solvent to good-solvent behavior of the matrix is predicted for $(M/M_0) > (P/M_0)^2$, where M_0 is the monomer molecular weight. The only modification necessary in eq 8 and 10 is to scale the hydrodynamic radius as the Flory radius R_{F}; i.e., $R(M) \sim R_{\mathrm{F}}(M) \sim M^{0.6}$. In P-chains short enough to be a good solvent for the M-chains, $D_{\mathrm{SE}} \sim M^{-0.6}$.

In a recent short communication[18] we demonstrated that the diffusion of long polystyrene (PS) M-chains in a P-chain PS melt is affected by the simultaneous diffusion of the neighboring P-chains provided that P is sufficiently small. These results were rationalized in terms of the Graessley model of constraint release. In this paper we extend this study in two respects. We give the results for the diffusion of a chain of $M = 2.0 \times 10^6$, which is twice as long as the longest chain used in our previous study. In addition we investigate the diffusion of these long M-chains into low molecular weight unentangled P-chain matrices ($P < M_{\mathrm{c}} \approx 2M_{\mathrm{e}}$). In such matrices we expect, and observe, that the P dependence of D^* is far weaker than for $P > M_{\mathrm{c}}$.

Experimental Procedure

Forward-recoil spectrometry was used to determine the concentration vs. depth profile of the M-chains that have diffused into a PS P-chain matrix. The molecular weights of the diffusing chains range from $M = 5.5 \times 10^4$ to 2.0×10^6. Except for the 2.0×10^6 molecular weight polymer all the M-chains were deuterated polystyrene (d-PS) and were diffused into undeuterated PS matrices of molecular weight P. The 2.0×10^6 molecular weight polymer was undeuterated PS, and it was diffused into d-PS P-chain matrices. For the two types of experiments the concentration vs. depth profiles of both deuterium and hydrogen were measured to obtain the volume fraction of the M-chain vs. depth. After diffusion the volume fraction of M-chain in each case was less than 0.1; i.e., the M-chains were dilute. Table I shows a list of the molecular weights and polydispersity indices of the polystyrenes used in the study.

The tracer diffusion coefficient D^* of the diffusing M-chain is determined by fitting the following solution of the diffusion equation to the experimental volume fraction vs. depth profile:

$$\phi(x) = \tfrac{1}{2}\{\mathrm{erf}\,[(h-x)/(4D^*t)^{1/2}] + \mathrm{erf}\,[(h+x)/(4D^*t)^{1/2}]\} \tag{11}$$

Table I
Weight-Average Molecular Weight and Polydispersity Indices of Various Polystyrene Fractions together with Their Sources

M_w	M_w/M_n	source
2 100	<1.06	Pressure Chemical Co.[a]
4 000	<1.06	Pressure Chemical Co.[a]
10 000	<1.06	Pressure Chemical Co.[a]
20 400	<1.06	Pressure Chemical Co.[a]
36 000	<1.06	Pressure Chemical Co.[a]
55 000	<1.06	Pressure Chemical Co.[a]
55 000	<1.06	Polymer Laboratories[b]
110 000	<1.06	Pressure Chemical Co.[a]
110 000	<1.1	Polymer Laboratories[b]
255 000	<1.06	Pressure Chemical Co.[a]
255 000	<1.1	Polymer Laboratories[b]
390 000	<1.06	Polymer Laboratories[b]
430 000	<1.1	Polymer Laboratories[b]
520 000	<1.1	Polymer Laboratories[b]
915 000	<1.1	Polymer Laboratories[b]
900 000	<1.06	Pressure Chemical Co.[a]
2 000 000	<1.2	Pressure Chemical Co.[a]
20 000 000	<1.3	Pressure Chemical Co.[a]

[a] PS. [b] d-PS.

where ϕ is the volume fraction and h is the initial thickness of the film of M-chains in contact with the thick matrix layer. Details of the experiment and analysis are outlined elsewhere.[9,10]

Results and Discussion

Diffusion of Long M-Chains in Entangled Matrices ($P < M_c$). Figure 1a shows a plot of D^* vs. P for a series of M-chains ranging from $M = 5.5 \times 10^4$ to 2×10^6. With the exception of the extreme molecular weights ($M = 5.5 \times 10^4$ and 2×10^6) all samples were diffused at 174 °C.[19] The diffusion of the $M = 5.5 \times 10^4$ and $M = 2 \times 10^6$ samples was carried out at 144 and 190 °C, respectively. All D^* values were corrected to a constant $T - T_g$ of 74 °C (constant free volume), where T_g is the glass transition temperature of the P-chain PS matrix. Allowance was made for the dependence of T_g on the molecular weight P of the matrix; i.e., for PS, $T_g = 100 - 1 \times 10^5/P$ (°C). The correction was made by using a WLF shift factor that has been found to describe the T dependence of D^*/T in PS.[20,21]

At large values of the molecular weight of the matrix, the D^* values are independent of P. This behavior is consistent with diffusion of the M-chain by reptation in a "fixed" environment of constraints. Below a characteristic molecular weight P^*, which slowly decreases with decreasing M, D^* increases rapidly as P decreases. This molecular weight P^* defines the point at which the diffusion coefficient due to reptation of the M-chains, D_{rep}, becomes comparable to the diffusion coefficient of the M-chains due to constraint release.

The solid lines drawn through the data in Figure 1a were computed by using eq 3, which represents the prediction of the constraint release model of Graessley.[3] Values of $z = 3.5$ and $M_e = 18000$[22] were used. Figure 1b shows the same data and the prediction of the nonindependent constraint release model of Klein[5] (eq 5) as dashed lines. The K parameter in the Klein model was adjusted for the best fit; a value of $K = 5.45$ was used.

As Figure 1 suggests, the two models, the constraint release model of Graessley[3] and the (nonindependent) constraint release model of Klein,[5] fit the experimental data within the precision of the measurement (~±20% of D^*). More elaborate procedures, involving subtracting D_{rep} from D^* and plotting the logarithm of the result vs. the logarithm of P to obtain the power law exponent for constraint release, lead to similar conclusions.[23] For the various M-chains the mean exponent found, -2.8 ± 0.3 (i.e., $(D^* - D_{rep}) \sim P^{-2.8}$), is almost midway between the -3 expected for constraint release and the -2.5 expected for nonindependent constraint release.

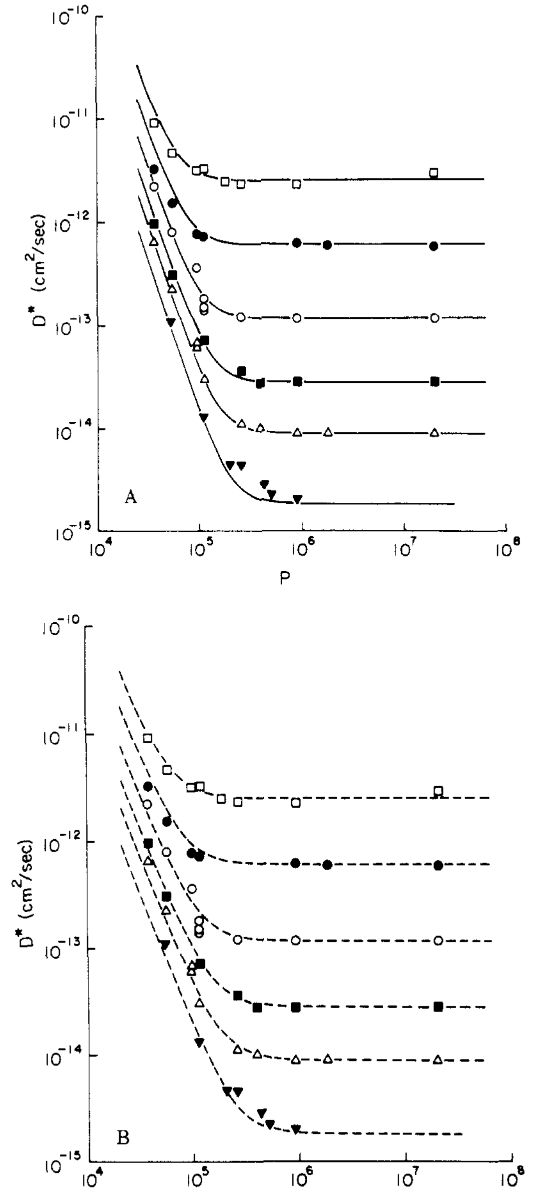

Figure 1. Tracer diffusion coefficient D^* of the M-chains as a function of the molecular weight P of the matrix. (a) The solid line is the constraint release model of Graessley (eq 3; values of $z = 3.5$ and $M_e = 18000$ were chosen). (b) The broken line is the nonindependent constraint release model of Klein (eq 5; $K = 5.45$). Diffusing chain molecular weights: (□) $M = 55000$; (●) $M = 110000$; (○) $M = 255000$; (■) $M = 520000$; (△) $M = 915000$; (▼) $M = 2000000$.

The M dependence of $(D^* - D_{rep})$ can be estimated by using a similar procedure to be $(D^* - D_{rep}) \sim M^{-0.8\pm0.1}$, reasonably close to the M^{-1} scaling predicted by both constraint release models. The Stokes–Einstein mechanism is not consistent with these results since the dependence of $(D^* - D_{rep})$ on M is larger than the $M^{-1/2}$ dependence predicted. Our failure to observe Stokes–Einstein diffusion for $P > M_c$ is consistent with Klein's prediction[5] that this behavior ought to be observed in the entangled regime only for M-chains of molecular weight much greater than $P(M_e/M_0)^2$.

At this point we prefer the Graessley model of constraint release, whose adjustable parameter z has a well-defined

Table II
Glass Transition Temperature (T_g), Fractional Free Volume at T_g (f_g), and Temperature (T) at Which the Fractional Free Volume of Each Polymer Matrix of Molecular Weight P Is Equal to the Same Value of 0.042

P	T_g, °C	f_g	T,[a] °C
2 000	58	0.023	90
4 000	77	0.026	104
10 000	88	0.026	116
20 400	93	0.027	119
20 000 000	100	0.028	125

[a] For f = 0.042.

physical meaning, simply on aesthetic grounds. The value of $z = 3.5$ required to produce the fit seems reasonable, since z cannot be much less than 3 and is unlikely to be greater than 5. Graessley and Struglinski[24,25] have found that a value of $z \approx 3$ is required to fit viscoelastic data on mixtures of polybutadienes.

Measurements of the viscoelasticity of melts of PS blends by Montfort and co-workers[26] yield results that are qualitatively consistent with ours. They find that the relaxation time τ' due to the effects of the matrix varies as $\tau' \sim M^{1.9}P^{2.3}$. From this result the matrix contribution to the diffusion of the M molecular weight chain should be $(D^* - D_{\text{rep}}) \sim M^{-0.9}P^{-2.3}$, a somewhat weaker dependence on P than we observe.

Recent measurements by Antonietti, Coutandin, and Sillescu[27] of tracer diffusion in PS P-chain melts using a forced Rayleigh scattering technique are in qualitative agreement with ours for M-chains that are relatively short, up to $M \simeq 110\,000$. Because they were restricted to relatively short M-chains, however, they were unable to observe the strong dependence of D^* on P we see for the longer M-chains in the constraint release regime.

Smith and co-workers[28] have reported the results of pattern fluorescence reappearance after photobleaching experiments on poly(propylene oxide) melts where matrix effects were observed. They report a dependence of D^* on P for P's above M_c that is much weaker than that we observed. These discrepancies may result because the dye molecule used to label their diffusing chain affects its motion, but it is difficult to understand how the label could affect the motion of the unlabeled matrix chains. Their study did not extend to P's where diffusion occurred purely by reptation, so a further comparison between our experiments and theirs is not possible.

Diffusion of Long M-Chains in Unentangled Matrices ($P < M_c$). It is well-known from viscoelastic measurements on unentangled PS melts[29-37] that it is important to correct to constant free volume because both T_g, the glass transition temperature, and $\alpha_f = \alpha_l - \alpha_g$, the thermal expansion coefficient of free volume, are functions of P in this range. Here α_l and α_g are the bulk thermal coefficients of expansion of the liquid and glass, respectively. Accordingly, these measurements of D^* were made by diffusing the polymers at different temperatures where the fractional free volume f[34] for each P-chain matrix is calculated to be equal to the same value of $f = 0.042$. The methods used in the calculations of f are shown in the Appendix. Table II shows a list of the matrix molecular weights together with their corresponding values of T_g and f_g, the fractional free volume at T_g. The table also shows the temperatures at which the experiments were conducted.

Figure 2 shows the dependence of the tracer diffusion coefficient D^* of the M-chain on the matrix molecular weight P in the range of molecular weights $P \leq 20\,000$. These are well below M_c, which is 35 000 for PS. The results of a least-squares analysis of these data are listed in Table III. The data are well described by

$$D^* \sim P^{-1} \qquad (12)$$

a dependence on P which is much weaker than that for $P > M_c$.

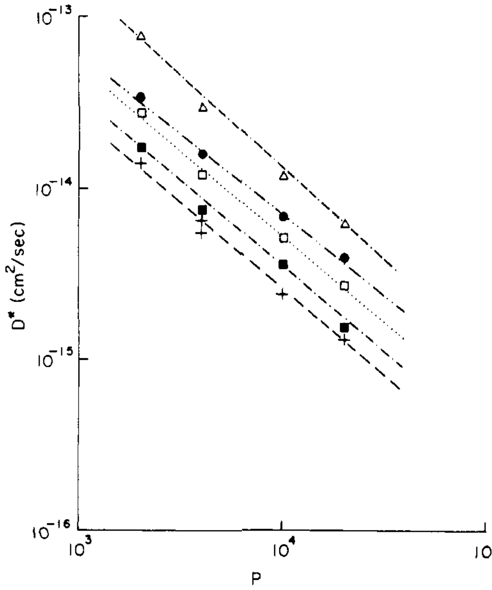

Figure 2. tracer diffusion coefficient of the M-chain diffusing into low molecular weight matrices $P < M_c$. Diffusing chain molecular weights: (△) M = 55 000; (●) M = 110 000; (□) M = 255 000; (■) M = 520 000; (+) M = 915 000.

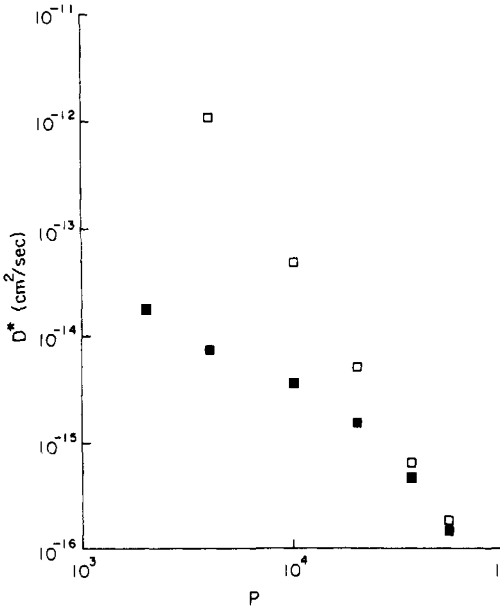

Figure 3. Tracer diffusion coefficient D^* of a chain of molecular weight M = 520 000 as a function of the molecular weight P of the matrix ($P < M_c$) at a constant fractional free volume of 0.042 (■) and at a constant temperature of 125 °C (□).

Table III
Dependence of D^* of Various M-Chains on the Matrix Molecular Weight P at Constant Fractional Free Volume

M	D^*, cm²/s	M	D^*, cm²/s
55 000	$P^{-1.1\pm0.1}$	520 000	$P^{-1.0\pm0.1}$
110 000	$P^{-0.9\pm0.1}$	915 000	$P^{-1.0\pm0.1}$
255 000	$P^{-1.0\pm0.1}$		

[a] For constant f = 0.042.

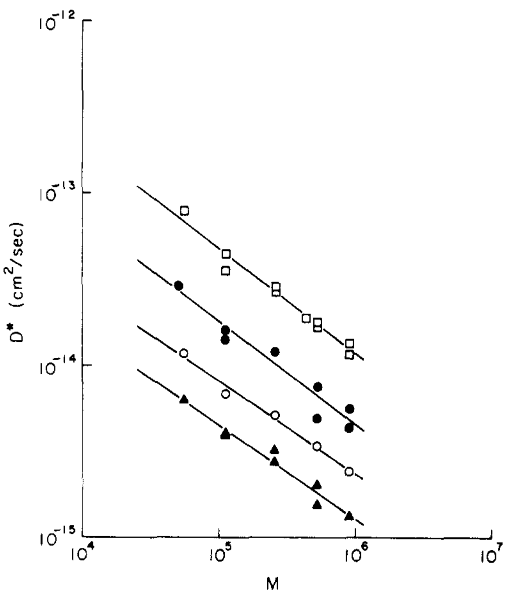

Figure 4. Tracer diffusion coefficient D^* of the M-chain as a function of its molecular weight for various matrices of molecular weight P less than M_c: (□) $P = 2000$; (●) $P = 4000$; (○) $P = 10\,000$; (▲) $P = 20\,000$).

Table IV
Dependence of D^* on M for a Given Host Molecular Weight at Various Temperatures for $P < M_c$

P	T,[a] °C	D^*, cm^2/s
2 000	90	$M^{-0.61\pm0.04}$
4 000	104	$M^{-0.60\pm0.07}$
10 000	116	$M^{-0.53\pm0.04}$
20 400	119	$M^{-0.55\pm0.04}$

[a] Diffusion temperature.

Tracer diffusion experiments conducted at constant temperature rather than at constant free volume lead to substantially different, and misleading, results regarding the dependence of D^* on P. D^* values for a chain of $M = 5.2 \times 10^5$ diffusing into various matrices at a constant temperature of $T = 125$ °C[38] are shown in Figure 3 as open squares. At this temperature the fractional free volume of a high molecular weight PS matrix is 0.042. These results are compared with those obtained at different temperatures where the fractional free volume of each matrix is 0.042. They are plotted as filled symbols in Figure 3. The slope of the data at constant T is substantially higher than that of the data at constant free volume. Hence the correction to constant free volume is obviously very important. The importance of this correction for self-diffusion of short chains has also been emphasized by von Meerwall and co-workers.[39]

The dependence of D^* on the molecular weight of the M-chain diffusing into a P-chain matrix (P is constant) is shown in Figure 4. Each line represents a least-squares fit to the data. The squares represent D^* values for diffusion into a matrix of $P = 2000$, the filled circles for $P = 4000$, the open circles for $P = 10\,000$, and the filled triangles for $P = 20\,000$. The data for the $P = 2000$ matrix were taken at three different temperatures (90, 92, and 95 °C) and then normalized to 90 °C. The data for the $P = 4000$ matrix were taken at 105 and 107 °C and normalized to 105 °C, and those for the $P = 20\,000$ matrix were taken at 119 and 121 °C and then normalized to 119 °C. Table IV contains information concerning the results of the least-squares fit to each set of data. These results show that D^* varies approximately as $M^{-(0.5-0.6)}$. The higher values of the exponent were observed for the shorter P-chain matrices. It follows that the diffusion coefficient of an M-chain into an unentangled P molecular weight matrix scales as

$$D^* = D_{\mathrm{uSE}} \sim P^{-1}M^{-(0.5-0.6)} \qquad (13)$$

in rough agreement with eq 10.

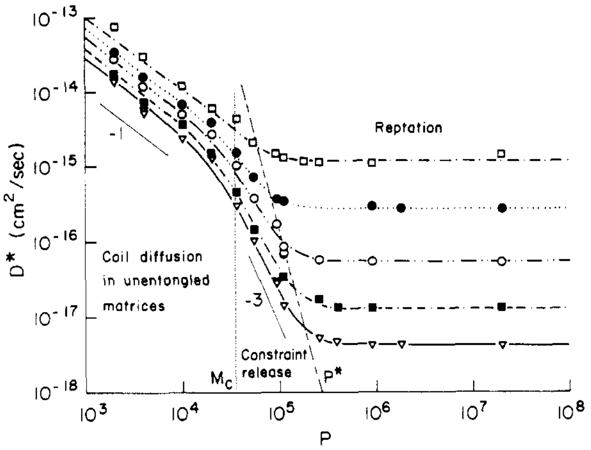

Figure 5. Dependence of tracer diffusion coefficient D^* on matrix molecular weight at a constant fractional free volume of 0.042. The matrix molecular weights range from below to above M_c: (□) $M = 55\,000$; (●) $M = 110\,000$; (○) $M = 255\,000$; (■) $M = 520\,000$; (▽) $M = 915\,000$).

Evidently hydrodynamic interactions between segments of the diffusing chain, as discussed in the model of Zimm,[17] are not screened; hence, the motion of the chain is non free draining. These results agree with the experiments of Smith et al. for tracer diffusion in their lowest molecular weight matrix[28] but are quite different from the results when the matrix comprises chains of molecular weight $P > M_c$. In this case the motion seems to be free draining, and consequently the Rouse model applies. It appears that the entanglements effectively screen intrachain hydrodynamic interactions.

The increase in the exponent of M as P decreases (Table IV) is intriguing since it may indicate a transition from Θ-solvent to good-solvent behavior of the matrix. According to theory,[2] P-chains less than $(M_0M)^{1/2}$ should show good-solvent behavior. For P-chains of our lowest molecular weight, 2000, this criterion is fulfilled for all the M-chains, whereas it is only fulfilled for M-chains greater than 160 000 for $P = 4000$ and is not fulfilled for any M-chains for the longer chain matrices, $P = 10\,000$ and 20 400. The exponent is approximately 0.6 for the two lowest P's, whereas it is approximately 0.54 for the highest P's. Unfortunately, the scatter in the D^* data precludes a more definitive test of the theoretical predictions at this time.

Summary

Figure 5 summarizes the matrix effects observed in the tracer diffusion of polystyrene.[40] There are three regimes, depending on the length of the P-chains. In the range of matrix molecular weights greater than $P^*(M)$, the motion of the M molecular weight chain occurs by reptation and is described by

$$D^* = D_0M^{-2}$$

In this regime D^* is independent of matrix molecular weight.

For values of P less than $P^*(M)$ but greater than M_c there is an additional contribution to the diffusion of the chain due to the constraint release process, and D^* increases with decreasing P approximately as

$$D^* = D_0(\alpha_{cr} M_e^2 M^{-1} P^{-3} + M^{-2})$$

In contrast, when the matrix molecular weight is below M_c, the diffusion mechanism becomes much less sensitive to P, increasing only as P^{-1}. Here the M-chain diffuses like a coil in a viscous medium ($\eta \sim P$) with a diffusion coefficient

$$D^* = D_{00} M^{-(0.5-0.6)} P^{-1}$$

where D_{00} is a constant.

The dependence of D^* on M in the constraint release regime suggests that the entangled matrix chains effectively screen the hydrodynamic interactions between M-chain segments so that the chain diffuses as a Rouse tube. In contrast, for $P < M_c$ the observed scaling ($D^* \sim M^{-(0.5-0.6)}$) implies that here the hydrodynamic interactions between segments of the M-chain are unscreened so the chain diffuses as a Zimm coil.

Acknowledgment. The financial support of this research by the NSF–DMR Polymers Program under Grant DMR-8303174 is gratefully acknowledged. P. F. Green received partial support in the form of a Public Health Service Pre-doctoral Fellowship. We also benefited from the use of the facilities of the Cornell Materials Science Center, which is funded by the DMR–MRL program of the NSF. We especially thank J. W. Mayer for his encouragement and helpful discussions. Useful ideas were contributed by W. W. Graessley, C. Cohen, P. J. Mills, C. J. Palmstrøm, and J. Klein.

Appendix

The parameters in Table II were determined as follows. One can define[34] the fractional free volume as $f = v_f/v_g$, where v_g is the difference between the specific volume, v, and the so-called occupied volume, v_0. The temperature dependence of f can be expressed as[34]

$$f = f_g + \alpha_f(T - T_g) \tag{A1}$$

Here $f_g = (v - v_0)/v_g$ is the fractional free volume at T_g (constant for high molecular weight polymers). It becomes appreciably dependent on molecular weight for low molecular weight polystyrenes. Fox and Flory[32] have shown that v_g can be expressed empirically as

$$v_g = 0.943 + 2.4 \times 10^{-4} T_g \tag{A2}$$

Others[31] have found the same dependence within the limits of experimental error. The occupied volume has been determined by Williams[29] from the data of Fox and Flory and is a constant for molecular weights above 15 000. The parameter α_f is the thermal expansion coefficient of the free volume and is also a function of molecular weight for polystyrenes in the molecular weight range 10^3–10^4. It can be approximated as[34]

$$\alpha_f = v_g^{-1} \alpha_l \tag{A3}$$

where $\alpha_l = \mathrm{d}v/\mathrm{d}T$ is the thermal expansion coefficient of the polymer in the liquid state. Here it is implicitly assumed that the expansion coefficient of the occupied volume α_0 is negligible in comparison. Alternative definitions assume that $\alpha_f = \alpha_l - \alpha_g$, where α_0 is considered to be parallel to α_g. This definition yields slightly different absolute values for f (a value of 0.036 for high molecular weight matrices), but since we are concerned with relative differences in f and since α_g is independent of molecular weight, this matter is of no concern in the temperature range of interest. The dependence of α_l on molecular weight is accurately given by[29,30]

$$\alpha_l = (5.5 + 643/M) \times 10^{-4} \tag{A4}$$

The final parameter of concern is T_g. The T_g values for the 2000, 4000, and 10 000 molecular weights were determined by differential scanning calorimetry. The others were calculated by using the equation $T_g = 100 - 1 \times 10^5/M$. These values are consistent with those reported by other authors.[30,33] Alternative calculations where one defines a relative free volume[27,34] as $f' = (v - v_0)/v_0$ and where $\alpha_f = v_0^{-1}\,\mathrm{d}v/\mathrm{d}T$ yield values of f' which differ from f by less than a few percent.

Registry No. PS (homopolymer), 9003-53-6.

Supplementary Material Available: Diffusion coefficients from Figure 1 at 174 °C and from Figure 5 at 125 °C (4 pages). Ordering information is given on any current masthead page.

References and Notes

(1) de Gennes, P.-G. *J. Chem. Phys.* **1971**, *55*, 572.
(2) de Gennes, P.-G. "Scaling Concepts in Polymer Physics"; Cornell University Press: Ithaca, NY, 1978; p 223.
(3) Graessley, W. W. *Adv. Polym. Sci.* **1982**, *47*, 67.
(4) Klein, J. *Polym. Prepr. (Am. Chem. Soc., Div. Polym. Chem.)* **1979**, *22*, 105.
(5) Klein, J. *Macromolecules* **1986**, *19*, 105.
(6) Daoud, M.; de Gennes, P.-G. *J. Polym. Sci., Polym. Phys. Ed.* **1979**, *17*, 1971.
(7) Doi, M.; Edwards, S. F. *J. Chem. Soc., Faraday Trans. 2* **1978**, 1798.
(8) Green, P. F.; Palmstrøm, C. J.; Mayer, J. W.; Kramer, E. J. *Macromolecules* **1985**, *18*, 501.
(9) Mills, P. J.; Green, P. F.; Palmstrøm, C. J.; Mayer, J. W.; Kramer, E. J. *Appl. Phys. Lett.* **1984**, *45*, 9.
(10) Green, P. F.; Kramer, E. J. *Polymer*, in press.
(11) Klein, J. *Nature (London)* **1978**, *271*, 143.
(12) Klein, J.; Briscoe, C. *Proc. R. Soc. London, A* **1979**, *365*, 53.
(13) Bartels, C. R.; Crist, B.; Graessley, W. W. *Macromolecules* **1984**, *17*, 2702.
(14) Antonietti, M.; Coutandin, J.; Sillescu, H. *Makromol. Chem., Rapid Commun.* **1984**, *5*, 525.
(15) Antonietti, A.; Coutandin, J.; Grutter, R.; Sillescu, H. *Macromolecules* **1984**, *17*, 798.
(16) Rouse, P. E. *J. Chem. Phys.* **1953**, *21*, 1272.
(17) Zimm, B. *J. Chem. Phys.* **1956**, *24*, 269.
(18) Green, P. F.; Mills, P. J.; Palmstrøm, C. J.; Mayer, J. W.; Kramer, E. J. *Phys. Rev. Lett.* **1984**, *53*, 2145.
(19) Earlier reports[9,18] gave this temperature erroneously as 170 °C; a subsequent recalibration of the oven shows it to have been 174 °C.
(20) Green, P. F.; Kramer, E. J. *J. Mater. Res.*, in press.
(21) Nemoto, N.; Landry, I. N.; Yu, H. *Polym. Commun.* **1985**, *25*, 141.
(22) Graessley, W. W. *Adv. Polym. Sci.* **1974**, *16*, 1.
(23) Green, P. F. Ph.D. Thesis, Cornell University, Ithaca, NY, 1985, pp 108–114.
(24) Graessley, W. W. *Faraday Symp. Chem. Soc.* **1983**, *18*, 7.
(25) Struglinski, M. J. Doctoral Dissertation, Northwestern University, 1984.
(26) Montfort, J. P.; Marin, G.; Monge, P. *Macromolecules* **1984**, *17*, 1551.
(27) Antonietti, M.; Coutandin, J.; Sillescu, H. *Macromolecules*, in press.
(28) Smith, B. A.; Samulski, E. T.; Yu, L. P.; Winnik, M. A. *Phys. Rev. Lett.* **1984**, *52*, 45; *Macromolecules* **1985**, *18*, 1901.
(29) Williams, M. L. *J. Appl. Phys.* **1958**, *29*, 1395.
(30) Fox, T. G.; Loshaek, S. *J. Polym. Sci.* **1955**, *15*, 371.
(31) Ueberreiter, K.; Kanig, G. *J. Colloid. Sci.* **1953**, *7*, 569.
(32) Fox, T. G.; Flory, P. J. *J. Appl. Phys.* **1950**, *21*, 581.
(33) Klein, J. *Contemp. Phys.* **1979**, *20*, 611.
(34) Ferry, J. D. "Viscoelastic Properties of Polymers", 3rd ed.; Wiley: New York, 1981.
(35) Rudin, A.; Burgin, D. *Polymer* **1975**, *16*, 291.
(36) Plazek, D. J. *J. Phys. Chem.* **1965**, *69*, 3481.
(37) Berry, G. C.; Fox, T. G. *Adv. Polym. Sci.* **1968**, *5*, 261.
(38) The measurements were performed at 131 °C and scaled to 125 °C by using the WLF equation, i.e., $\log [D^*(T_1)T_2/D^*(T_2)T_1] = C_1(T_1 - T_2)/[C_2 + (T_1 - T_2)]$.

(39) von Meerwall, E.; Grigsby, J.; Tomich, D.; von Antwerp, R. *J. Polym. Sci., Polym. Phys. Ed.* **1982**, *20*, 1037.
(40) The data were obtained by scaling the results shown in Figure 1 to a temperature of 125 °C. We calculated the fractional free volume to be equal to 0.042 (the same value calculated for the low molecular weight matrices (see Appendix)) for higher molecular weight matrix chains at this temperature. The shift factor was obtained by scaling the data to results obtained for the diffusion of a $M = 110000$ molecular weight chain in a matrix of 2.0×10^6 at this temperature.

Further Morphological Studies of *trans*-1,4-Polyisoprene Crystallized from Solution

Jia-rui Xu and Arthur E. Woodward*

Department of Chemistry, City University of New York, City College, New York, New York 10031. *Received October 2, 1985*

ABSTRACT: Three fractions of *trans*-1,4-polyisoprene with $M_v = (1.4\text{–}5.9) \times 10^5$ were crystallized from amyl acetate solution at temperatures from 0 to 30 °C. Optical microscopy before drying and scanning electron microscopy after treatment in suspension with OsO_4 and drying were used to investigate these preparations. Changes in morphology with molecular weight and crystallization temperature were followed; curved lamellas, lamellar stacks, and spherulites were found. Scanning electron microscopy revealed features, such as lamellar interpenetration and curvature, branching, and twisting, either not seen or not seen clearly with optical microscopy. When stacks of curved lamellas are subjected to ultrasonic vibration, preferential fracture across the center portion of all the layers takes place.

Introduction

trans-1,4-Polyisoprene (TPI) can be crystallized in monoclinic (α)[1] or orthorhombic (β)[2] forms depending on the conditions used. Seeded crystallization from solution, a process that involves dissolution at elevated temperature, precipitation, redissolution at moderate temperatures, and crystallization at constant temperature, is found usually to yield overgrown α-form TPI lamellas.[3,4] On the other hand, direct crystallization from solution, consisting of dissolution at an elevated temperature followed by isothermal crystallization, leads to more complex structures, such as sheaves, spherulites, and curved lamellar aggregates, which can be in the α- or β-forms depending on the crystallization solvent and temperature.[5] The various structures resulting from direct crystallization from solution were previously studied in suspension prior to drying[5] with interference contrast optical microscopy. As is usually the case with optical micrographs, the magnification and contrast were low and therefore few details of the lamellar organization were visible. However, in that work transmission electron microscopy was successfully employed to view at much higher magnifications a preparation of curved lamellar aggregates that had been reacted with OsO_4 while in suspension prior to drying. Due to their overall thickness and complexity sheaves and spherulites are difficult to investigate by transmission electron microscopy. However, as shown below, it is possible to study these structures with scanning electron microscopy. In order to preserve the organization of these structures while in suspension prior to drying while enhancing the contrast, reaction with OsO_4 is carried out. That the overall appearance of these structures is not modified by the chemical treatment is evident by comparing interference contrast optical micrographs taken of them in suspension with scanning electron micrographs of similar fields taken after reaction and drying.

In the work presented here direct crystallization at 0–30 °C was carried out with fractions of synthetic *trans*-1,4-polyisoprene with viscosity-average molecular weights of 1.4×10^5, 2.6×10^5, and 5.9×10^5, extending the range of the previous study to higher molecular weights. Also in the present work the effects of ultrasonic vibration of sheave and spherulite structures, prior to OsO_4 treatment and drying, were investigated.

Experimental Section

Samples. Synthetic *trans*-1,4-polyisoprene (TPI) was obtained from Polychemicals, Inc. This was found earlier with gel permeation chromatography[6] to have $M_n = 3.5 \times 10^4$, $M_w/M_n = 4.8$, and a trans-1,4 content from carbon-13 NMR of 99%.

TPI fractions were obtained by fractional precipitation from toluene solution with methanol using the scheme shown in Figure 1. The three fractions P_5, P_6, and P_{15} were used. Viscosity-average molecular weights of 1.4×10^5, 2.6×10^5, and 5.9×10^5, respectively, were determined by solution viscosity measurements in toluene at 30 °C employing the relationship $[\eta] = 3.34 \times 10^{-2} M^{0.686}$. This relationship was determined by using molecular weight fractions with $M_w/M_n = 1.2\text{–}1.3$ prepared on a diatomaceous earth column and characterized by gel permeation chromatography earlier.[4,5]

Crystallization. Samples were prepared from 0.1 and 1% (w/v) amyl acetate solutions by the direct method. The polymer was dissolved in amyl acetate by heating to 90–95 °C for 30 min; the solution was cooled to 60 °C and then placed in a constant-temperature bath at one of the following temperatures: 0, 10, 20, or 30 °C for 1 h to 4 days. One preparation was obtained by a seeded crystallization.[5]

Optical Microscopy. After crystallization of the sample, a drop of the amyl acetate suspension was placed on a slide with a cover glass and viewed at room temperature with a Zeiss photomicroscope having interference contrast optics.

Scanning Electron Microscopy. The TPI–amyl acetate suspensions were mixed with OsO_4 for about 1 h and washed with fresh amyl acetate. A drop was placed on aluminum foil; the sample was dried and then coated with evaporated Au/Pd(80/20). For a number of the preparations the suspension was placed in an ultrasonic vibrator for 3 min prior to the chemical treatment. A Cambridge Stereoscan S4 scanning electron microscope was used for viewing these preparations.

Results

For TPI with $M_v = 1.4 \times 10^5$ direct crystallization at 20 °C from 1% amyl acetate was carried out for 1, 2, 3, 5, 24, and 48 h followed by treatment with OsO_4 before drying. For crystallization times up to 3 h relatively little precipitation occurs. A scanning electron micrograph of one

0024-9297/86/2219-1114$01.50/0